Title

A Small-Molecule Wnt Mimic Improves Human Limbal Stem Cell Ex Vivo Expansion.

Permalink

https://escholarship.org/uc/item/5s70n1zv

Journal

iScience, 23(5)

ISSN

2589-0042

Authors

Zhang, Chi
Mei, Hua
Robertson, Sarah YT
et al.

Publication Date
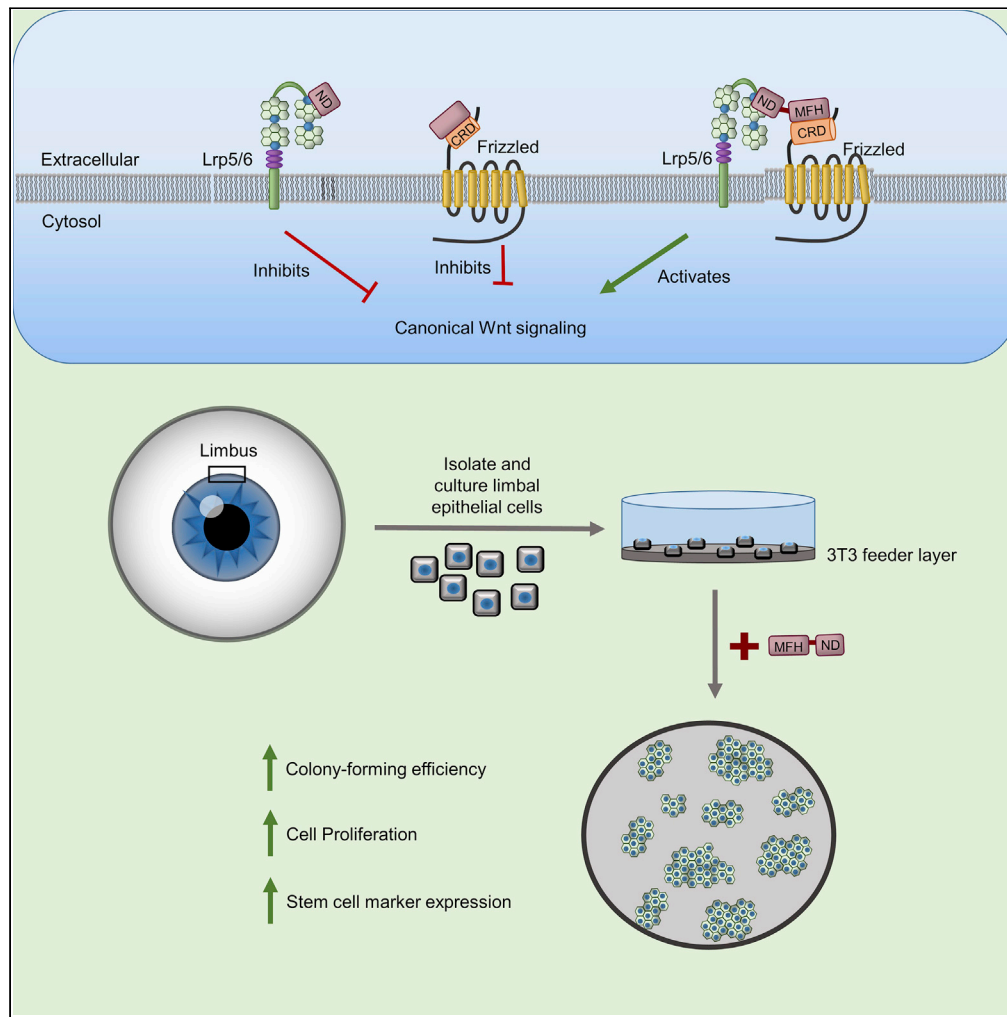
2020-05-01

DOI

10.1016/j.isci.2020.101075

Peer reviewed

Article

A Small-Molecule Wnt Mimic Improves Human Limbal Stem Cell *Ex Vivo* Expansion

Chi Zhang, Hua Mei, Sarah Y.T. Robertson, Ho-Jin Lee, Sophie X. Deng, Jie J. Zheng

deng@jsei.ucla.edu (S.X.D.)
jzheng@jsei.ucla.edu (J.J.Z.)

HIGHLIGHTS

MFH-ND is generated by linking a Frizzled inhibitor and an LRP5/6 inhibitor

MFH-ND activates the canonical Wnt pathway by oligomerizing Frizzled and LRP5/6

MFH-ND improves the stem cell phenotype of cultivated limbal epithelial cells

MFH-ND has therapeutic potential to improve limbal stem cell deficiency treatment

Article

A Small-Molecule Wnt Mimic Improves Human Limbal Stem Cell *Ex Vivo* Expansion

Chi Zhang,[1,4] Hua Mei,[2,4] Sarah Y.T. Robertson,[1,4] Ho-Jin Lee,[3] Sophie X. Deng,[1,*] and Jie J. Zheng[1,5,*]

SUMMARY

Ex vivo **cultured limbal stem/progenitor cells is an effective alternative to other surgical treatments for limbal stem cell deficiency, but a standard xenobiotic-free method for culturing the LSCs** *in vitro* **needs to be optimized. Because Wnt ligands are required for LSC expansion and preservation** *in vitro*, **to create a small-molecule Wnt mimic, we created a consolidated compound by linking a Wnt inhibitor that binds to the Wnt co-receptor Frizzled to a peptide derived from the N-terminal Dickkopf-1 that binds to Lrp (low-density lipoprotein receptor-related protein) 5/6, another Wnt co-receptor. This Wnt mimic not only enhances cellular Wnt signaling activation, but also improves the progenitor cell phenotype of** *in vitro* **cultured limbal epithelial cells. As the maintenance of stem cell characteristics in the process of culture expansion is essential for the success of ocular surface reconstruction, the small molecules generated in this study may be helpful in the development of pharmaceutical reagents for treating corneal wounds.**

INTRODUCTION

The integrity of the corneal epithelium, the outermost layer of the cornea, is crucial to maintaining healthy vision. Corneal epithelial cells regularly slough off and detach through blinking but are replenished by the centripetal migration and differentiation of stem/progenitor cells in the limbal region surrounding the cornea, known as limbal stem cells (LSCs) (Dua et al., 2000, 2005; Figueira et al., 2007; Meek and Knupp, 2015; Nowell and Radtke, 2017; Secker and Daniels, 2008; Thoft et al., 1989; Yazdanpanah et al., 2017). Having an insufficient population of LSCs leads to a pathological state called limbal stem cell deficiency (LSCD), in which the surrounding conjunctiva invades the cornea, obstructing vision (Dua et al., 2000; Haagdorens et al., 2016). The type of intervention depends on the severity of LSCD and whether one eye (unilateral) or both eyes (bilateral) are affected. Because these patients lack a sufficient LSC population, full corneal transplants are contraindicated in patients with LSCD (Holland et al., 2003). Therefore, LSC transplantation in the form of a keratolimbal allograft from a cadaveric donor is the standard treatment, especially in bilateral disease cases (Holland et al., 2003). In the case of unilateral disease, a keratolimbal autograft from the patient's healthy eye has a high survival rate (Basu et al., 2016; Haagdorens et al., 2016; Kenyon and Tseng, 1989). However, keratolimbal allografts have a high graft rejection rate and keratolimbal autografts pose significant danger to the patient's healthy eye (Haagdorens et al., 2016; Sasamoto et al., 2018).

An effective alternative to these surgeries is to remove a small limbal explant from the patient, use this explant to seed an *ex vivo* culture of limbal epithelial cells (LECs) that contain LSCs, and transplant the cell sheet back into the patient (Bobba et al., 2015; Ezhkova and Fuchs, 2010; Gonzalez et al., 2017; Haagdorens et al., 2016). *Ex vivo* LSC expansion utilizes a patient's own limbal tissue, thereby minimizing the risk of damage to the healthy eye and graft rejection, and does not require significant cellular reprogramming as in studies using other stem cell sources (Sasamoto et al., 2018). Currently, the standard for culturing LECs *ex vivo* involves culturing the LECs on a bed of NIH-3T3 feeder cells, which provide structural support and a variety of growth factors to allow proliferation and preservation of the LSC population (Pellegrini et al., 1997). Because NIH3T3cells are derived from mouse embryonic fibroblasts, a xenobiotic-free alternative is required to eliminate possible xenogenic contaminants and translate *ex vivo* expanded LECs to the clinic in the United States (Pellegrini et al., 2016). Therefore, it is imperative to understand the mechanical and

[1]Stein Eye Institute, Department of Ophthalmology, David Geffen School of Medicine at UCLA, Los Angeles, CA 90095, USA

[2]Department of Ophthalmology, University of North Carolina School of Medicine, Chapel Hill, NC 27517, USA

[3]Department of Natural Sciences, Southwest Tennessee Community College, Memphis, TN 38134, USA

[4]These authors contributed equally

[5]Lead Contact

*Correspondence:
deng@jsei.ucla.edu (S.X.D.),
jzheng@jsei.ucla.edu (J.J.Z.)

https://doi.org/10.1016/j.isci.2020.101075

growth factor requirements for LSCs cultured *ex vivo* to develop a new standard xenobiotic-free LEC culture system for future LSCD treatment.

We have previously found that Wnt signaling, an integral component of many stem cell processes including proliferation, renewal, differentiation, survival, quiescence, and polarity (Clevers and Nusse, 2012; Gomez-Orte et al., 2013; Katoh and Katoh, 2007; Komiya and Habas, 2008; Lien and Fuchs, 2014; Loh et al., 2016; Nusse and Clevers, 2017; Nusse et al., 2008), is a requirement for the preservation of LSCs in culture (Gonzalez et al., 2019). Wnt ligands are growth factors that can influence the cell cycle to not only affect cell proliferation, but also contribute to cytoskeleton arrangement and therefore give directionality to cell proliferation and regulate spatial growth (Loh et al., 2016; Niehrs and Acebron, 2012; Nusse and Clevers, 2017). In the canonical Wnt signaling pathway, secreted Wnt ligand binds to the LRP5/6 coreceptor and the GPCR (G protein-coupled receptor)-like membrane coreceptor Frizzled (Fzd), allowing Fzd and LRP5/6 to oligomerize and pass the Wnt signal into the cell (Dann et al., 2001; Hua et al., 2018; Schulte and Wright, 2018; Tran and Zheng, 2017). Canonical Wnt molecules and inhibitors have been shown to be differentially expressed in the limbal epithelium and LSC niche *in vivo* (Dziasko and Daniels, 2016; Kulkarni et al., 2010; Nakatsu et al., 2013). It has also been demonstrated that canonical Wnt signaling is crucial for the *in vitro* proliferation and preservation of LSCs (Di Girolamo et al., 2015; Mei et al., 2014; Nakatsu et al., 2011).

Because Wnt ligands are critical factors that NIH-3T3 feeder cells provide to sustain the LECs, it is theoretically possible to treat the LECs with recombinant Wnt ligands. Wnt ligands are highly hydrophobic and require detergents to purify, presenting challenges to effectively generate and study the therapeutic potential of recombinant Wnt ligands (Janda et al., 2017; Janda and Garcia, 2015; Willert and Nusse, 2012; Willert, 2008). Efforts to modulate Wnt signaling therefore focus on the coreceptors LRP5/6 and Fzd and their interactions with Wnt ligands and regulatory molecules (Ahadome et al., 2017; Gonzalez et al., 2019; Janda et al., 2017; Li et al., 2012; Tran and Zheng, 2017). In the present study, we present a small-molecule approach to mimic Wnt ligand-induced oligomerization of LRP5/6 and Fzd. We show that the peptide derived from the N-terminal region of DKK1 (Dickkopf WNT signaling pathway inhibitor) (termed as ND) that binds to the first propeller domain of LRP5/6 and a small molecule (termed as MFH) that binds to the CRD (cysteine-rich domain) domain of Fzd separately reduced progenitor cell properties in cultured LECs. However, a consolidated molecule linking MFH and ND together acts as a canonical Wnt mimic by inducing oligomerization of LRP5/6 and Fzd to activate Wnt signaling. The MFH-ND molecule also enhanced LSC expansion *in vitro*. This study provides evidence that generating small molecules that mimic growth factors required for LSC preservation and expansion is a feasible xenobiotic-free alternative to the NIH-3T3 feeder layer.

RESULTS

Compound MFH Inhibits Wnt Signaling by Binding to the Cysteine-Rich Domain of Fzd

The N-terminal extracellular domain of Fzd has a cysteine-rich domain (CRD) that interacts with secreted Wnt proteins (Dann et al., 2001). The crystal structures of the CRD of FZD8 (FZD8-CRD) in complex with glycosylated Wnt8 (Chu et al., 2013; Janda et al., 2012) and of FZD8-CRD in complex with lysine-methylated and deglycosylated human Wnt3 (Hirai et al., 2019) are available. The Wnt8/FZD8-CRD complex structure shows that the Wnt-binding mode resembles a hand grasping the CRD at two opposing sites, site 1 and site 2. Site 1 is a lipid-binding site; in the Wnt8/FZD8-CRD complex, site 1 binds to palmitoleic acid that attached to Ser189 of Wnt8. Site 2 is located in the C-terminal region of the CRD and is involved in the direct protein-protein interaction (mostly hydrophobic interactions) with the bound Wnt molecule. Site 1 is highly conserved in the Fzd family, and site 2 is thought to be responsible for discriminating between specific Wnt/CRD pairs as demonstrated in mutagenesis studies (Bazan et al., 2012; Dann et al., 2001).

Using a hybrid, structure-based, lead discovery approach that combined molecular modeling, biophysical methods, and a cell-based assay, we identified a set of small-molecule inhibitors targeting the site 2 of FZD8 CRD (Lee et al., 2015). Through structure-based screening, we obtained a small molecule from the ChemDiv database, 4-[2-[[9E]-2,7-dimethoxy-9H-fluoren-9-ylidene]hydrazin-1-yl]benzoic acid (Figure 1A, we term it as MFH). Using ^{1}H-^{15}N heteronuclear single quantum coherence (HSQC) NMR, we showed that MFH binds to the FZD8-CRD (Figure S1). The 293STF (HEK293 cell line expressing firefly luciferase under the control of the TCF/LEF promoter) cell line, which expresses firefly luciferase under the control of the
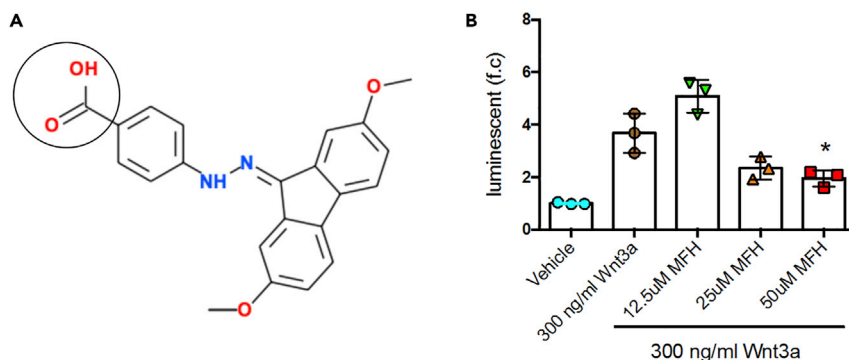
Figure 1. Compound MFH Inhibits Wnt Signaling by Binding to the Cysteine-Rich Domain of Fzd

(A) The sequence of the broad-spectrum Wnt inhibitor MFH. The circled region shows the methoxy residue that will be coupled to the ND peptide to generate the Wnt mimic small molecule MFH-ND.

(B) Stable transfected 293STF cells expressing firefly luciferase under the control of the TCF/LEF promoter were treated with vehicle; 300 ng/mL Wnt3a; and 300 ng/mL Wnt3a with 12.5, 25, and 50 μM MFH. After 16 h, Wnt3a-induced luciferase activities in 293STF cells were detected using One-Glo and Tox kit (Promega). Data are represented as means ± SEM. *p < 0.05 relative to Wnt3a treatment (n = 3).

See also Figures S1 and S2.

TCF/LEF (T cell factor/lymphoid enhancer-binding factor) promoter, was used to examine the activation or inhibition effect of the small molecules on regulating the canonical Wnt signaling pathway. We found that MFH indeed inhibited Wnt signaling (Figure 1B) as measured by the 293STF cells. The 293STF cells also showed that the IC50 of MFH is approximately 25 μM and that MFH does not affect the luminescence of the 293STF cells in the absence of Wnt (Figure S2).

A Consolidated Small Molecule that Binds Both LRP5/6 and Fzd Functions as a Wnt Mimic

Figure 2B shows a simplified model of the interaction of Wnt ligand with LRP5/6 and Fzd. We hypothesized that a small molecule that mimics Wnt ligand could be generated by linking two different small molecules: one that binds to Fzd (blocks the interaction between Wnt and Fzd) and one that binds LRP5/6 (blocks the interaction between Wnt and LRP5/6), respectively. Because MFH has a free carboxyl group, through this group, we coupled MFH to the N terminus of a peptide derived from N-terminal region of DKK that binds to the first β-propeller domain of LRP6 (Bourhis et al., 2011). The N-terminal LRP5/6 interaction motif of DKK (Asn-X-Ile/Val [NXI/V], where X is any amino acid) is present in all LRP5/6-binding Wnt inhibitors, including DKK1, DKK2, DKK4, and SOST (sclerostin) (Ahn et al., 2011; Bourhis et al., 2011). The complex structures with the DKK1 or SOST peptide containing this motif revealed the binding of the peptides to the top center of the first β-propeller domain of LRP5/6. The sequences of the DKK1 and SOST peptides that bound to the first β-propeller of LRP6 in the crystal structures are NS**N**AIKN and LP**N**AIGR, respectively (Bourhis et al., 2011), where Asn(3) and Ile(5) are the key residues in the interaction. Based on structural information (Bourhis et al., 2011), we chose the ND peptide, SNAIK, derived from N-terminal DKK1 as a potential LRP5/6-binding peptide. We then placed a pentaethylene glycol ((PEG)$_5$) spacer between the two molecules and termed this bivalent molecule as MFH-ND (Figure 2A).

In the 293STF cell-based reporter assay, we found that MFH-ND slightly activates canonical Wnt signaling without exogenous Wnt at a concentration of 50 μM (Figure S3). Similarly, in the 3T3 cell-based reporter assay, MFH-ND augmented Wnt3a-activated canonical Wnt activity dependent on the concentrations of Wnt3a and MFH-ND (Figure S4). In the presence of 300 ng/mL Wnt3a, MFH-ND dramatically enhanced Wnt signaling. MFH-ND and MFH showed a dose-dependent activation and inhibition, respectively, on Wnt3a-activated canonical Wnt Activity (Figure 2C). ND showed no significant effect on the Wnt3a-activated canonical Wnt Activity (Figure 2C).

The Wnt Mimic Small Molecule Increases Colony-Forming Efficiency and Proliferation of Expanded Limbal Stem/Progenitor Cells *In Vitro*

Freshly isolated limbal stem/progenitor cells (LSCs) were cultured with 5, 10, and 20 μM of small molecules (MFH-ND, MFH, and ND) for 11–13 days. Proliferation rate was used as a measure of the
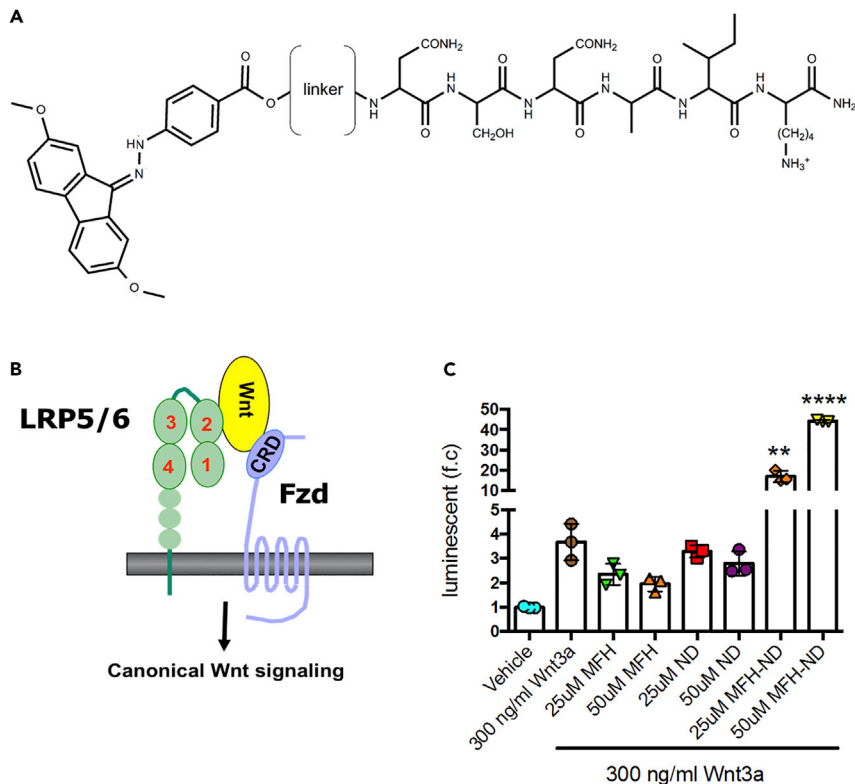
Figure 2. A Consolidated Small Molecule that Binds Both Lrp5/6 and Fzd Mimic Wnt Ligand Functions as a Wnt Mimic

(A) Sequence of Wnt mimic MFH-ND molecule. The portion to the left of the linker corresponds to MFH, whereas the portion to the right of the linker corresponds to the ND peptide. Linker: $(PEG)_5$.

(B) Schematic of canonical Wnt signaling activation via Wnt ligand-induced oligomerization of Fzd and Lrp5/6. The Wnt mimic is designed to bind to the first β-propeller domain of Lrp5/6 and the CRD domain of Fzd, thereby oligomerizing the two coreceptors.

(C) Stable transfected 293STF cells expressing luciferase under control of the TCF/LEF promoter were treated with vehicle; 300 ng/mL Wnt3a; 300 ng/mL Wnt3a with 25 and 50 μM each of MFH-ND, MFH, or ND. After 16 h, Wnt3a-induced luciferase activities in 293STF cells were evaluated using One-Glo and Tox kit (Promega). **$p < 0.01$, and ****$p < 0.0001$ relative to Wnt3a treatment (n = 3).

Data are represented as means ± SEM. See also Figure S3.

proliferative capacity of the progenitor cell population. LSCs cultured with different concentrations of MFH-ND and ND showed compact cuboidal stem-cell morphology, which was comparable with the cells without treatment (control) (Figure 3A). MFH at 5 μM caused vacuole-like structures in cultured LSCs; MFH at 10 and 20 μM failed to support the growth of LSCs and caused the death of 3T3 feeder cells (Figure 3A). MFH-ND at tested concentrations generated 32%–48% more LSCs (Figure 3D) than control, whereas ND showed no effect on cell proliferation (Figure 3D). MFH at 5 μM tended to decrease cell proliferation, and MFH at 10 and 20 μM inhibited cell proliferation significantly by more than 98% (Figure 3D).

The colony-forming efficiency (CFE), which is a classic parameter for epithelial stem cells, was measured at the end of culture. Because CFE counts the individual progenitor cells that are capable of forming discrete colonies, CFE is a widely accepted method of functional analysis of the clonogenic capacity of the progenitor cell population. The CFEs of LSCs cultured in 5, 10, and 20 μM MFH-ND were significantly (17%–21%) higher than that of the control; CFEs for LSCs in 10 and 20 μM MFH were significantly (80%–95%) lower than that of the control; ND did not alter the CFE (Figures 3B and 3C). Because 10 and 20 μM MFH failed to generate enough cells for cellular analysis, these two conditions were excluded from further characterization of stem-cell properties.
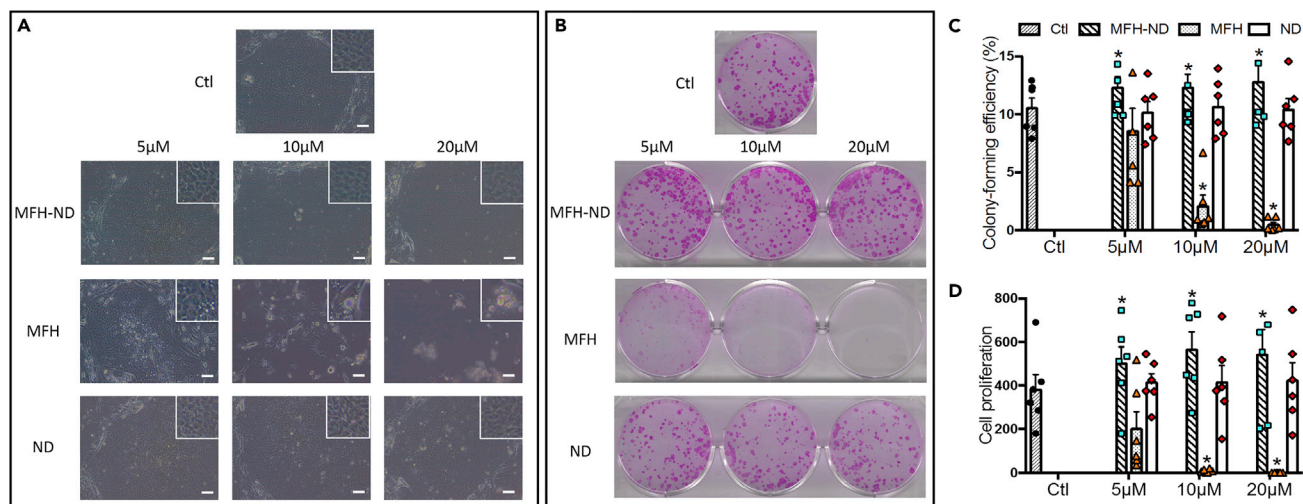
Figure 3. The Wnt Mimic Small Molecule Increases Colony-Forming Efficiency and Proliferation of Expanded Limbal Stem/Progenitor Cells (LSCs) *In Vitro*

(A) Representative morphology images of LSCs co-cultured with different concentrations of Wnt small molecules. The insert shows an enlarged area within each colony. Scale bar: 50 μM.

(B) Representative CFE pictures of LSCs co-cultured with different concentrations of Wnt small molecules.

(C) Quantitative analysis of CFE data. CFE was calculated as the number of colonies divided by the number of cells seeded. *: $p \leq 0.05$ in comparison with result of control (Ctl).

(D) Cell proliferation of LSCs co-cultured with different concentrations of Wnt small molecules. Cell proliferation was calculated as the total number of cells harvested divided by the number of cells seeded.

Data are represented as means $\pm$ SEM. *: $p \leq 0.05$ in comparison with result of control (Ctl) (n = 6 independent donors).

The Wnt Mimic Small Molecule Enhances Additional Stem-Cell Properties of Expanded LSCs *In Vitro*

Additional stem-cell properties of LSCs, including small cell size (cell diameter ≤ 12 μm), expressions of putative stem/progenitor markers (p63α and cytokeratin 14 [K14]), and expression of maturation marker (cytokeratin 12 [K12]), were examined in the expanded cells. MFH-ND showed no effect on the percentage of small cells at tested concentrations (Figure 4A), whereas it significantly increased the absolute number of small cells at 10 μM (Figure 4E). MFH showed no effect on the percentage of small cells or the absolute number of small cells (Figures 4A and 4E). ND tended to decrease the percentage of small cells from 5 to 20 μM; at 10 μM it significantly decreased the percentage of small cells by 69% (Figure 4A). ND did not show significant impact on the absolute number of small cells (Figure 4E).

MFH-ND tended to increase the percentage of p63α-bright cells from a lower concentration (5 μM) to a higher concentration (20 μM); it significantly increased the percentage of p63α-bright cells to 29% at 20 μM when compared with the 14% in the control (Figure 4B). As MFH-ND increased LSC proliferation, this trend was more robust for the absolute number of p63α-bright cells. MFH-ND at 10 and 20 μM was able to generate 137 to 144 p63α-bright cells per cell seeded, whereas the control generated 42 p63α-bright cells per cell seeded (Figure 4F). MFH at 5 μM did not alter the percentage of p63α-bright cells. However, it significantly reduced the absolute number of p63α-bright cells possibly owing to its inhibition on cell proliferation (Figures 4B and 4F). ND at 5 and 10 μM did not affect the percentage or the absolute number of p63α-bright cells; ND at 20 μM significantly reduced the percentage of p63α-bright cells to 7% compared with 14% in the control (Figures 4B and 4F). ND at 20 μM did not show significant impact on the absolute number of p63α-bright cells (Figure 4F).

MFH-ND, MFH, and ND did not affect the percentage of cytokeratin (K) 14^{+} cells at tested concentrations (Figure 4C). Compared with the control, which generated 369 K14^{+} cells per cell seeded, MFH-ND at 5, 10, and 20 μM significantly increased the absolute number of K14^{+} cells to 487–545 cells per cell seeded; MFH at 5 μM decreased the absolute number of K14^{+} cells significantly to 179 K14^{+} cells per cell seeded; ND did not affect the absolute number of K14^{+} cells at tested concentrations (Figure 4G).
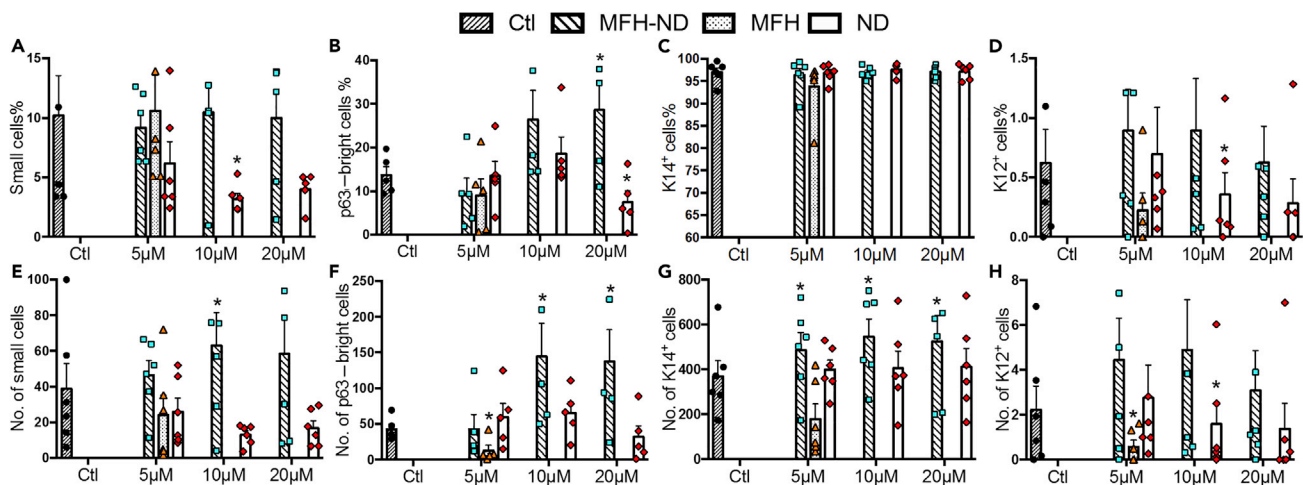
Figure 4. The Wnt Mimic Small Molecule Enhances Additional Stem-Cell Properties of Expanded LSCs *In Vitro*

(A and E) Quantification of the percentage and absolute number of small cells, defined as cell diameter ≤12 μm. The cell diameters were manually measured by ImageJ.

(B and F) The percentage and absolute number of p63α-bright cells in cultured LECs. The absolute number of p63α-bright cells = the percentage of p63α-bright cells x (number of cells harvested/number of cells seeded).

(C and G) The percentage and absolute number of K14+ cells in LSCs co-cultured with different concentrations of Wnt small molecules. The absolute number of K14+ cells = the percentage of K14+ cells x (number of cells harvested/number of cells seeded).

(D and H) The percentage and absolute number of K12+ cells in LSCs co-cultured with different concentrations of Wnt small molecules. The absolute number of K12+ cells = the percentage of K12+ cells x (number of cells harvested/number of cells seeded).

Data are represented as means ± SEM. *: p ≤ 0.05 in comparison with result of control (Ctl) (n = 5 independent donors). See also Table S1.

MFH-ND and MFH did not alter the percentage of K12+ (differentiated) cells, whereas ND tended to decrease the percentage of K12+ cells (Figure 4D). ND at 10 μM significantly decreased the percentage of K12+ (differentiated) cells to 0.4% compared with 0.6% in the control (Figure 4D). MFH-ND showed no effect on the absolute number of K12+ cells at tested concentrations (Figure 4H). MFH at 5 μM and ND at 10 μM significantly decreased the absolute number of K12+ cells (Figure 4H).

DISCUSSION

Like other Fzd-binding molecules (Lee et al., 2015), the Fzd inhibitor MFH identified in this study also inhibits Wnt signaling transduction by blocking the interaction between Wnt ligands and Fzd receptors. MFH completely ablated the expansion of LECs at high concentrations, confirming our previous conclusion that Wnt signaling is a key regulator of LEC survival and growth (Gonzalez et al., 2019). The N-terminal DKK peptide ND binds to the first β-propeller domain of LRP6 (Bourhis et al., 2011). We did not observe significant inhibition of canonical Wnt signaling measured by the 293STF cells with any concentration of ND, despite the putative inhibitive effect of ND on Wnt binding to LRP5/6. Because the first β-propeller domain only binds to a small set of Wnt ligands (Bao et al., 2012; Gong et al., 2010; Joiner et al., 2013), ND likely cannot completely block canonical Wnt signaling. This could explain a weak inhibition trend of ND on canonical Wnt signaling activation as measured by the 293STF cells and the lack of significant differences in LEC morphology, proliferation, or CFE in low concentrations of ND. Nevertheless, 20 μM ND significantly decreased the percentage of p63α-bright cells, suggesting high concentrations of ND may be able to inhibit LSC proliferation. This result is consistent with one of our earlier studies that showed IC15, a potent Wnt inhibitor that binds to LRP5/6, causes significant decreases in proliferation and CFE (Gonzalez et al., 2019). Nevertheless, compared with ND or IC15, we found that MFH could more effectively eliminate the ability of *ex vivo* LSC expansion and the ability of 3T3s to support *ex vivo* LSC expansion. Unlike ND or IC15, MFH binds to the CRD domain of Fzd and blocks both canonical and non-canonical Wnt signaling. Therefore, the data suggest that not only canonical Wnt signaling, but also non-canonical Wnt signaling can support a low level of LSC proliferation and survival. Similarly, it has been shown in other systems that β-catenin signaling could occur separately from canonical Wnt signaling (Arnsdorf et al., 2009; Thrasivoulou et al., 2013).

By physically linking the two Wnt inhibitors, MFH and ND, we generated the consolidated molecule MFH-ND. MFH-ND enhances Wnt signaling presumably by inducing the oligomerization of two Wnt

coreceptors, LRP5/6 and Fzd. Consistent with the notion that Wnt is important in LSC preservation *in vitro*, all concentrations of MFH-ND studied increased LEC proliferation, colony forming efficiency, and the number of undifferentiated K14+ LECs, which reflect an increase in the progenitor cell population in culture. The high variation between each donor tissue may make the significance in these increases difficult to appreciate; however, MFH-ND consistently improves the progenitor cell phenotype in the LECs when compared with the control for each donor. The highest concentration of MFH-ND additionally increased the number and percentage of p63α-bright LECs, a factor that correlates strongly with the success of a limbal transplant in patients with LSCD (Gonzalez et al., 2018; Rama et al., 2010). These results suggest that MFH-ND supports the proliferation of undifferentiated and progenitor cells. Owing to the presence of autocrine Wnt ligand secreted by the cultured LECs or paracrine Wnt ligand secreted by the 3T3 feeder cells, it is likely that MFH-ND supports the activity of these endogenous Wnt ligands rather than activating Wnt signaling independently of the secreted Wnt ligands. This conclusion is supported in that MFH-ND significantly upregulated the canonical pathway activation in the 293STF cell assay in the presence of Wnt3a ligand but warrants further investigation to confirm in the LEC culture.

The concept of phenocopying Wnt signaling by inducing complex formation between LRP5/6 and Fzd has been reported (Chen et al., 2020; Gonzalez et al., 2019; Janda et al., 2017; Tao et al., 2019). MFH-ND similarly aims to promote oligomerization of Wnt ligand co-receptors LRP5/6 and Fzd. Although MFH-ND alone does not significantly increase Wnt signaling activation, it upregulates the pathway in the presence of Wnt ligand suggesting the compound enhances Wnt signaling by aiding Wnt signalosome assembly (Gammons and Bienz, 2018; Hirai et al., 2019). MFH-ND alone may be insufficient to oligomerize Fzd and LRP5/6 because ND binds to the first propeller domain of LRP5/6, which is farthest from the membrane in the extracellular domain, and may not force LRP5/6 into close proximity with Fzd enough to induce Wnt signalosome formation (Bourhis et al., 2011; Joiner et al., 2013). Therefore, it seems that MFH-ND requires additional Wnt ligand to upregulate Wnt signaling. However, the design of the consolidated Wnt mimic has much room to improve. For example, the length of the linker region connecting MFH and ND can be optimized or ND can be replaced with a molecule that targets a different β-propeller domain of LRP5/6. Moreover, future studies could use hybrid structure-based and cellular assays to generate small molecules that target the subtle differences at site 2 of specific Fzd CRD domains. We previously showed that FZD7 was differentially expressed in the LSC population (Mei et al., 2014), so the proposed methods could be used to specifically induce LRP5/6 oligomerization with FZD7. The concept of the Wnt mimic MFH-ND and the methods presented here are a valuable resource to stem cell research behind the LSC *ex vivo* expansion.

Ex vivo LSC expansion and transplantation is a promising treatment for LSCD because it utilizes a patient's own limbal tissue, thereby minimizing the risk of damage to the healthy eye and graft rejection, and does not require significant cellular reprogramming as in studies using other stem cell sources (Sasamoto et al., 2018). Success of *ex vivo* cultured LEC transplants depends on the quality and quantity of LSC population in the culture. The cells must cover the corneal surface, retain some proliferative capacity, and maintain a progenitor cell phenotype to support the progenitor cell population in the patient (Gonzalez et al., 2018, 2019; Mariappan et al., 2010; Pellegrini et al., 2013; Rama et al., 2010; Sejpal et al., 2013; Shortt et al., 2011). In pursuit of a xenobiotic-free alternative to NIH-3T3 feeder cells, human amniotic membrane (HAM) has been implemented. However, HAM usage requires thorough donor screening, is difficult to standardize owing to donor variation in physical properties and biological activity, and involves intensive *in vitro* processing (Connon et al., 2010; Gicquel et al., 2009; Haagdorens et al., 2019; Lopez-Valladares et al., 2010; Mariappan et al., 2010; Massie et al., 2015). On the other hand, matrix components isolated from HAM have been useful in identifying niche signaling factors involved in regulating LSC expansion and preventing LSC differentiation, including the balance between Wnt and BMP (bone morphogenic protein) signaling (Chen et al., 2015; Han et al., 2014; Tseng, 2016). Developing a xenobiotic-free culture system without the need for additional allogeneic donor materials would eliminate complications arising from culturing LECs on 3T3 feeder cells or HAM. This system would require additional factors that are capable of activating the pathways required for LSC preservation and proliferation and a scaffold on which to grow the LECs. Indeed, recently, a collagen-based hydrogel system was used to culture LECs *in vitro* (Haagdorens et al., 2019), demonstrating the possibility of generating a xenobiotic-free and human donor material-free system using a similar scaffold given the proper combination of growth factors and small molecules. Engineering a small-molecule Wnt protein mimic is a crucial step toward generating a cocktail of necessary niche factors for an optimal *in vitro* expansion of LSCs.

Limitations of the Study

MFH-ND appears to have little activity independent of Wnt ligand, so the structure of MFH-ND will need to be further optimized and its mechanism investigated. Nevertheless, studying MFH-ND is a proof of concept that activating the canonical Wnt pathway via oligomerization of Fzd and LRP5/6 improves the progenitor cell phenotype of cultured LECs.

METHODS

All methods can be found in the accompanying Transparent Methods supplemental file.

SUPPLEMENTAL INFORMATION

Supplemental Information can be found online at https://doi.org/10.1016/j.isci.2020.101075.

AUTHOR CONTRIBUTIONS

Conceptualization, J.J.Z., S.X.D.; Methodology, J.J.Z., S.X.D., C.Z., H.M., and H.-J.L.; Investigation, C.Z., H.M., and H.-J.L.; Writing – Original Draft, S.Y.T.R. and H.M.; Writing – Review & Editing, S.Y.T.R., C.Z., and J.J.Z.; Funding Acquisition, S.X.D. and J.J.Z.; Resources, S.X.D. and J.J.Z.; Supervision, S.X.D. and J.J.Z.

DECLARATION OF INTERESTS

The authors declare no competing interests.

REFERENCES

Ahadome, S.D., Zhang, C., Tannous, E., Shen, J., and Zheng, J.J. (2017). Small-molecule inhibition of Wnt signaling abrogates dexamethasone-induced phenotype of primary human trabecular meshwork cells. Exp. Cell Res. 357, 116–123.

Ahn, V.E., Chu, M.L., Choi, H.J., Tran, D., Abo, A., and Weis, W.I. (2011). Structural basis of Wnt signaling inhibition by Dickkopf binding to LRP5/6. Dev. Cell 21, 862–873.

Arnsdorf, E.J., Tummala, P., and Jacobs, C.R. (2009). Non-canonical Wnt signaling and N-cadherin related beta-catenin signaling play a role in mechanically induced osteogenic cell fate. PLoS One 4, e5388.

Bao, J., Zheng, J.J., and Wu, D. (2012). The structural basis of DKK-mediated inhibition of Wnt/LRP signaling. Sci. Signal. 5, pe22.

Basu, S., Sureka, S.P., Shanbhag, S.S., Kethiri, A.R., Singh, V., and Sangwan, V.S. (2016). Simple limbal epithelial transplantation: long-term clinical outcomes in 125 cases of unilateral chronic ocular surface burns. Ophthalmology 123, 1000–1010.

Bazan, J.F., Janda, C.Y., and Garcia, K.C. (2012). Structural architecture and functional evolution of Wnts. Dev. Cell 23, 227–232.

Bobba, S., Chow, S., Watson, S., and Di Girolamo, N. (2015). Clinical outcomes of xeno-free expansion and transplantation of autologous ocular surface epithelial stem cells via contact lens delivery: a prospective case series. Stem Cell Res. Ther. 6, 23.

Bourhis, E., Wang, W., Tam, C., Hwang, J., Zhang, Y., Spittler, D., Huang, O.W., Gong, Y., Estevez, A., Zilberleyb, I., et al. (2011). Wnt antagonists bind through a short peptide to the first beta-propeller domain of LRP5/6. Structure 19, 1433–1442.

Chen, H., Lu, C., Ouyang, B., Zhang, H., Huang, Z., Bhatia, D., Lee, S.J., Shah, D., Sura, A., Yeh, W.C., et al. (2020). Development of potent, selective surrogate WNT molecules and their application in defining frizzled requirements. Cell Chem. Biol.

Chen, S.Y., Han, B., Zhu, Y.T., Mahabole, M., Huang, J., Beebe, D.C., and Tseng, S.C. (2015). HC-HA/PTX3 purified from amniotic membrane promotes BMP signaling in limbal niche cells to maintain quiescence of limbal epithelial progenitor/stem cells. Stem Cells 33, 3341–3355.

Chu, M.L., Ahn, V.E., Choi, H.J., Daniels, D.L., Nusse, R., and Weis, W.I. (2013). Structural Studies of Wnts and identification of an LRP6 binding site. Structure 21, 1235–1242.

Clevers, H., and Nusse, R. (2012). Wnt/beta-catenin signaling and disease. Cell 149, 1192–1205.

Connon, C.J., Doutch, J., Chen, B., Hopkinson, A., Mehta, J.S., Nakamura, T., Kinoshita, S., and Meek, K.M. (2010). The variation in transparency of amniotic membrane used in ocular surface regeneration. Br. J. Ophthalmol. 94, 1057–1061.

Dann, C.E., Hsieh, J.C., Rattner, A., Sharma, D., Nathans, J., and Leahy, D.J. (2001). Insights into Wnt binding and signalling from the structures of two Frizzled cysteine-rich domains. Nature 412, 86–90.

Di Girolamo, N., Bobba, S., Raviraj, V., Delic, N.C., Slapetova, I., Nicovich, P.R., Halliday, G.M., Wakefield, D., Whan, R., and Lyons, J.G. (2015). Tracing the fate of limbal epithelial progenitor cells in the murine cornea. Stem Cells 33, 157–169.

Dua, H.S., Saini, J.S., Azuara-Blanco, A., and Gupta, P. (2000). Limbal stem cell deficiency: concept, aetiology, clinical presentation, diagnosis and management. Indian J. Ophthalmol. 48, 83–92.

Dua, H.S., Shanmuganathan, V.A., Powell-Richards, A.O., Tighe, P.J., and Joseph, A. (2005). Limbal epithelial crypts: a novel anatomical

structure and a putative limbal stem cell niche. Br. J. Ophthalmol. 89, 529–532.

Dziasko, M.A., and Daniels, J.T. (2016). Anatomical features and cell-cell interactions in the human limbal epithelial stem cell niche. Ocul. Surf. 14, 322–330.

Ezhkova, E., and Fuchs, E. (2010). Regenerative medicine: an eye to treating blindness. Nature 466, 567–568.

Figueira, E.C., Di Girolamo, N., Coroneo, M.T., and Wakefield, D. (2007). The phenotype of limbal epithelial stem cells. Invest. Ophthalmol. Vis. Sci. 48, 144–156.

Gammons, M., and Bienz, M. (2018). Multiprotein complexes governing Wnt signal transduction. Curr. Opin. Cell Biol. 51, 42–49.

Gicquel, J.J., Dua, H.S., Brodie, A., Mohammed, I., Suleman, H., Lazutina, E., James, D.K., and Hopkinson, A. (2009). Epidermal growth factor variations in amniotic membrane used for ex vivo tissue constructs. Tissue Eng. Part A 15, 1919–1927.

Gomez-Orte, E., Saenz-Narciso, B., Moreno, S., and Cabello, J. (2013). Multiple functions of the noncanonical Wnt pathway. Trends Genet. 29, 545–553.

Gong, Y., Bourhis, E., Chiu, C., Stawicki, S., DeAlmeida, V.I., Liu, B.Y., Phamluong, K., Cao, T.C., Carano, R.A., Ernst, J.A., et al. (2010). Wnt isoform-specific interactions with coreceptor specify inhibition or potentiation of signaling by LRP6 antibodies. PLoS One 5, e12682.

Gonzalez, S., Chen, L., and Deng, S.X. (2017). Comparative study of xenobiotic-free media for the cultivation of human limbal epithelial stem/progenitor cells. Tissue Eng. Part C Methods 23, 219–227.

Gonzalez, S., Oh, D., Baclagon, E.R., Zheng, J.J., and Deng, S.X. (2019). Wnt signaling is required for the maintenance of human limbal stem/progenitor cells in vitro. Invest. Ophthalmol. Vis. Sci. 60, 107–112.

Gonzalez, G., Sasamoto, Y., Ksander, B.R., Frank, M.H., and Frank, N.Y. (2018). Limbal stem cells: identity, developmental origin, and therapeutic potential. Wiley Interdiscip. Rev. Dev. Biol. 7, https://doi.org/10.1002/wdev.303.

Haagdorens, M., Cepla, V., Melsbach, E., Koivusalo, L., Skottman, H., Griffith, M., Valiokas, R., Zakaria, N., Pintelon, I., and Tassignon, M.J. (2019). In vitro cultivation of limbal epithelial stem cells on surface-modified crosslinked collagen scaffolds. Stem Cells Int. 2019, 7867613.

Haagdorens, M., Van Acker, S.I., Van Gerwen, V., Ni Dhubhghaill, S., Koppen, C., Tassignon, M.J., and Zakaria, N. (2016). Limbal stem cell deficiency: current treatment options and emerging therapies. Stem Cells Int. 2016, 9798374.

Han, B., Chen, S.Y., Zhu, Y.T., and Tseng, S.C. (2014). Integration of BMP/Wnt signaling to control clonal growth of limbal epithelial progenitor cells by niche cells. Stem Cell Res. 12, 562–573.

Hirai, H., Matoba, K., Mihara, E., Arimori, T., and Takagi, J. (2019). Crystal structure of a mammalian Wnt-frizzled complex. Nat. Struct. Mol. Biol. 26, 372–379.

Holland, E.J., Djalilian, A.R., and Schwartz, G.S. (2003). Management of aniridic keratopathy with keratolimbal allograft: a limbal stem cell transplantation technique. Ophthalmology 110, 125–130.

Hua, Y., Yang, Y., Li, Q., He, X., Zhu, W., Wang, J., and Gan, X. (2018). Oligomerization of Frizzled and LRP5/6 protein initiates intracellular signaling for the canonical WNT/beta-catenin pathway. J. Biol. Chem. 293, 19710–19724.

Janda, C.Y., Dang, L.T., You, C., Chang, J., de Lau, W., Zhong, Z.A., Yan, K.S., Marecic, O., Siepe, D., Li, X., et al. (2017). Surrogate Wnt agonists that phenocopy canonical Wnt and beta-catenin signalling. Nature 545, 234–237.

Janda, C.Y., and Garcia, K.C. (2015). Wnt acylation and its functional implication in Wnt signalling regulation. Biochem. Soc. Trans. 43, 211–216.

Janda, C.Y., Waghray, D., Levin, A.M., Thomas, C., and Garcia, K.C. (2012). Structural basis of wnt recognition by frizzled. Science 337, 59–64.

Joiner, D.M., Ke, J., Zhong, Z., Xu, H.E., and Williams, B.O. (2013). LRP5 and LRP6 in development and disease. Trends Endocrinol. Metab. 24, 31–39.

Katoh, M., and Katoh, M. (2007). WNT signaling pathway and stem cell signaling network. Clin. Cancer Res. 13, 4042–4045.

Kenyon, K.R., and Tseng, S.C. (1989). Limbal autograft transplantation for ocular surface disorders. Ophthalmology 96, 709–722, discussion 722-703.

Komiya, Y., and Habas, R. (2008). Wnt signal transduction pathways. Organogenesis 4, 68–75.

Kulkarni, B.B., Tighe, P.J., Mohammed, I., Yeung, A.M., Powe, D.G., Hopkinson, A., Shanmuganathan, V.A., and Dua, H.S. (2010). Comparative transcriptional profiling of the limbal epithelial crypt demonstrates its putative stem cell niche characteristics. BMC Genomics 11, 526.

Lee, H.J., Bao, J., Miller, A., Zhang, C., Wu, J., Baday, Y.C., Guibao, C., Li, L., Wu, D., and Zheng, J.J. (2015). Structure-based Discovery of novel small molecule Wnt signaling inhibitors by targeting the cysteine-rich domain of frizzled. J. Biol. Chem. 290, 30596–30606.

Li, X., Shan, J., Chang, W., Kim, I., Bao, J., Lee, H.J., Zhang, X., Samuel, V.T., Shulman, G.I., Liu, D., et al. (2012). Chemical and genetic evidence for the involvement of Wnt antagonist Dickkopf2 in regulation of glucose metabolism. Proc. Natl. Acad. Sci. U S A 109, 11402–11407.

Lien, W.H., and Fuchs, E. (2014). Wnt some lose some: transcriptional governance of stem cells by Wnt/beta-catenin signaling. Genes Dev. 28, 1517–1532.

Loh, K.M., van Amerongen, R., and Nusse, R. (2016). Generating cellular diversity and spatial form: wnt signaling and the evolution of multicellular animals. Dev. Cell 38, 643–655.

Lopez-Valladares, M.J., Teresa Rodriguez-Ares, M., Tourino, R., Gude, F., Teresa Silva, M., and Couceiro, J. (2010). Donor age and gestational age influence on growth factor levels in human amniotic membrane. Acta Ophthalmol. 88, e211–216.

Mariappan, I., Maddileti, S., Savy, S., Tiwari, S., Gaddipati, S., Fatima, A., Sangwan, V.S., Balasubramanian, D., and Vemuganti, G.K. (2010). In vitro culture and expansion of human limbal epithelial cells. Nat. Protoc. 5, 1470–1479.

Massie, I., Kureshi, A.K., Schrader, S., Shortt, A.J., and Daniels, J.T. (2015). Optimization of optical and mechanical properties of real architecture for 3-dimensional tissue equivalents: towards treatment of limbal epithelial stem cell deficiency. Acta Biomater. 24, 241–250.

Meek, K.M., and Knupp, C. (2015). Corneal structure and transparency. Prog. Retin. Eye Res. 49, 1–16.

Mei, H., Nakatsu, M.N., Baclagon, E.R., and Deng, S.X. (2014). Frizzled 7 maintains the undifferentiated state of human limbal stem/progenitor cells. Stem Cells 32, 938–945.

Nakatsu, M.N., Ding, Z., Ng, M.Y., Truong, T.T., Yu, F., and Deng, S.X. (2011). Wnt/beta-catenin signaling regulates proliferation of human cornea epithelial stem/progenitor cells. Invest. Ophthalmol. Vis. Sci. 52, 4734–4741.

Nakatsu, M.N., Vartanyan, L., Vu, D.M., Ng, M.Y., Li, X., and Deng, S.X. (2013). Preferential biological processes in the human limbus by differential gene profiling. PLoS One 8, e61833.

Niehrs, C., and Acebron, S.P. (2012). Mitotic and mitogenic Wnt signalling. EMBO J. 31, 2705–2713.

Nowell, C.S., and Radtke, F. (2017). Corneal epithelial stem cells and their niche at a glance. J. Cell Sci. 130, 1021–1025.

Nusse, R., and Clevers, H. (2017). Wnt/beta-catenin signaling, disease, and emerging therapeutic modalities. Cell 169, 985–999.

Nusse, R., Fuerer, C., Ching, W., Harnish, K., Logan, C., Zeng, A., ten Berge, D., and Kalani, Y. (2008). Wnt signaling and stem cell control. Cold Spring Harb. Symp. Quant Biol. 73, 59–66.

Pellegrini, G., Lambiase, A., Macaluso, C., Pocobelli, A., Deng, S., Cavallini, G.M., Esteki, R., and Rama, P. (2016). From discovery to approval of an advanced therapy medicinal product-containing stem cells, in the EU. Regen. Med. 11, 407–420.

Pellegrini, G., Rama, P., Matuska, S., Lambiase, A., Bonini, S., Pocobelli, A., Colabelli, R.G., Spadea, L., Fasciani, R., Balestrazzi, E., et al. (2013). Biological parameters determining the clinical outcome of autologous cultures of limbal stem cells. Regen. Med. 8, 553–567.

Pellegrini, G., Traverso, C.E., Franzi, A.T., Zingirian, M., Cancedda, R., and De Luca, M. (1997). Long-term restoration of damaged corneal surfaces with autologous cultivated corneal epithelium. Lancet 349, 990–993.

Rama, P., Matuska, S., Paganoni, G., Spinelli, A., De Luca, M., and Pellegrini, G. (2010). Limbal stem-cell therapy and long-term corneal regeneration. N. Engl. J. Med. *363*, 147–155.

Sasamoto, Y., Ksander, B.R., Frank, M.H., and Frank, N.Y. (2018). Repairing the corneal epithelium using limbal stem cells or alternative cell-based therapies. Expert Opin. Biol. Ther. *18*, 505–513.

Schulte, G., and Wright, S.C. (2018). Frizzleds as GPCRs - more conventional than we thought! Trends Pharmacol. Sci. *39*, 828–842.

Secker, G.A., and Daniels, J.T. (2008). Limbal epithelial stem cells of the cornea. StemBook. https://doi.org/10.3824/stembook.1.48.1.

Sejpal, K., Ali, M.H., Maddileti, S., Basu, S., Ramappa, M., Kekunnaya, R., Vemuganti, G.K., and Sangwan, V.S. (2013). Cultivated limbal epithelial transplantation in children with ocular surface burns. JAMA Ophthalmol. *131*, 731–736.

Shortt, A.J., Tuft, S.J., and Daniels, J.T. (2011). Corneal stem cells in the eye clinic. Br. Med. Bull *100*, 209–225.

Tao, Y., Mis, M., Blazer, L., Ustav, M.J., Steinhart, Z., Chidiac, R., Kubarakos, E., O'Brien, S., Wang, X., Jarvik, N., et al. (2019). Tailored tetravalent antibodies potently and specifically activate Wnt/ Frizzled pathways in cells, organoids and mice. Elife *8*, e46134.

Thoft, R.A., Wiley, L.A., and Sundarraj, N. (1989). The multipotential cells of the limbus. Eye (Lond) *3* (Pt 2), 109–113.

Thrasivoulou, C., Millar, M., and Ahmed, A. (2013). Activation of intracellular calcium by multiple Wnt ligands and translocation of beta-catenin into the nucleus: a convergent model of Wnt/Ca2+ and Wnt/beta-catenin pathways. J. Biol. Chem. *288*, 35651–35659.

Tran, F.H., and Zheng, J.J. (2017). Modulating the wnt signaling pathway with small molecules. Protein Sci. *26*, 650–661.

Tseng, S.C. (2016). HC-HA/PTX3 purified from amniotic membrane as novel regenerative matrix: insight into relationship between inflammation and regeneration. Invest. Ophthalmol. Vis. Sci. *57*, ORSFh1-8.

Willert, K., and Nusse, R. (2012). Wnt proteins. Cold Spring Harb. Perspect. Biol. *4*, a007864.

Willert, K.H. (2008). Isolation and application of bioactive Wnt proteins. Methods Mol. Biol. *468*, 17–29.

Yazdanpanah, G., Jabbehdari, S., and Djalilian, A.R. (2017). Limbal and corneal epithelial homeostasis. Curr. Opin. Ophthalmol. *28*, 348–354.

Supplemental Information

A Small-Molecule Wnt Mimic

Improves Human Limbal

Stem Cell *Ex Vivo* Expansion

Chi Zhang, Hua Mei, Sarah Y.T. Robertson, Ho-Jin Lee, Sophie X. Deng, and Jie J. Zheng
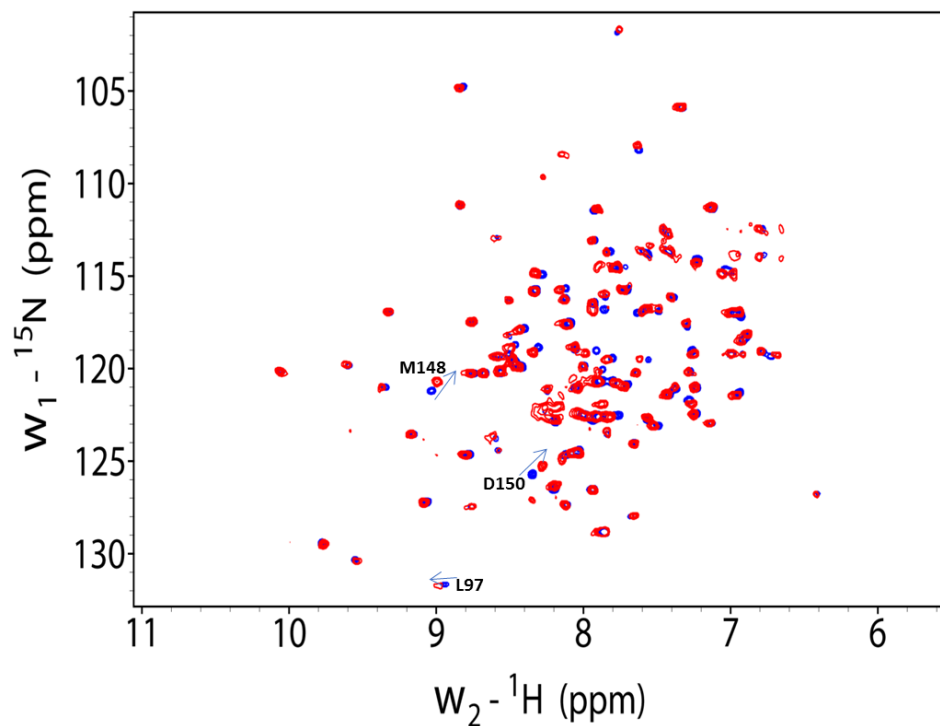
Supplemental Information

Figure S1: Structural analysis of compound MFH binding to FZD8 CRD. Related to Figure 1. Superposition of ^{1}H-^{15}N HSQC spectra of ^{15}N labeled FZD8 CRD in the absence of (blue) and presence of compound MFH (red). The FZD8 CRD was subcloned and transformed into Rosetta2 (DE3) cells. Target protein, FZD8 CRD, was expressed by cells cultured in MOPS media supplemented with [15N]ammonium chloride as the source of nitrogen. The protein was further purified by HPLC and maintained in 50 mM potassium phosphate at pH 6.5. Compound MFH was titrated into the solution of 50µM FZD8 CRD at a final concentration of 276µM. Upon titration, key residues (L97, M148 and D150) from protein binding site of FZD8 CRD showed chemical shift perturbation, indicating compound MFH specifically targets the interaction between FZD8 CRD and binding partner.
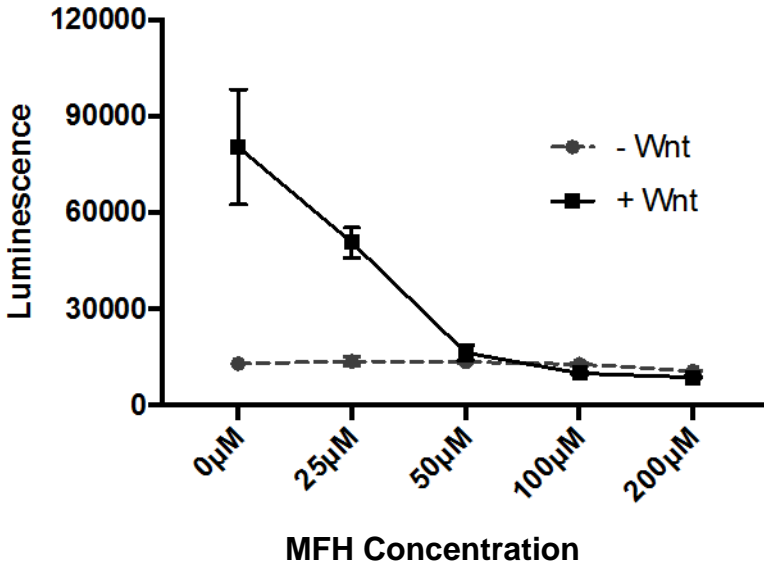
Figure S2: Wnt canonical pathway activation decreases with increasing concentrations of MFH. Related to Figure 1. 3T3 cells expressing firefly luciferase under the TCF/LEF promoter were treated with increasing concentrations of MFH in the presence (+ Wnt, solid black line) or absence (- Wnt, dotted gray line) of 300 ng/ml Wnt3a. (n = 2)
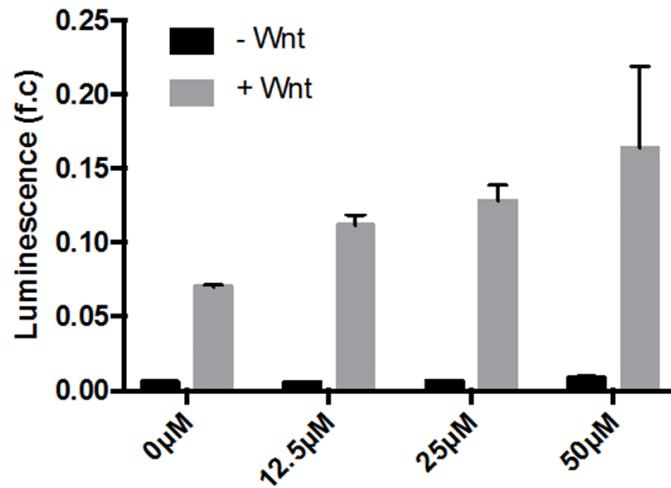
Figure S3: Wnt canonical pathway activation increases with increasing concentrations of MFH-ND and in the presence of Wnt3a. Related to Figure 2. 293STF cells, which express firefly luciferase under the TCF/LEF reporter, were treated with increasing concentrations of MFH-ND in the presence (+ Wnt, light gray bar) or absence (- Wnt, dark gray bar) of 300 ng/ml Wnt3a (n = 2).
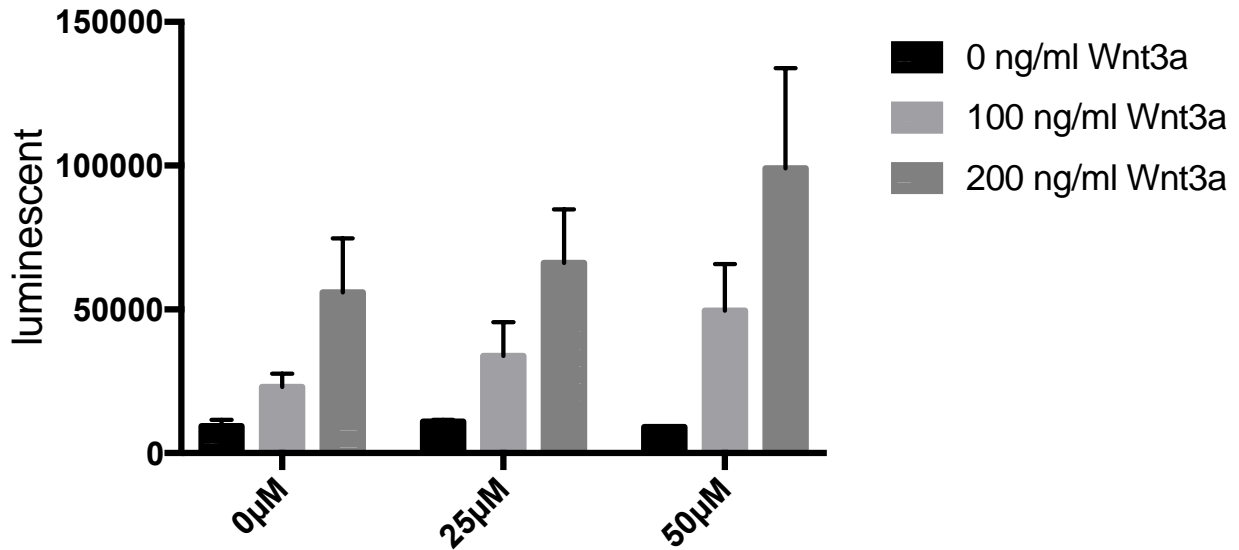
Figure S4: MFH-ND augments Wnt3a activity in a dose-dependent manner. Related to Figure 2. 3T3 cells expressing firefly luciferase under the TCF/LEF promoter were treated with 0 μM, 25 μM, or 50 μM of MFH-ND in the absence of Wnt3a (black bars), presence of 100 ng/ml Wnt3a (light gray bars), or presence of 200 ng/ml Wnt3a (dark gray bar). (n = 2)

Table S1: Primary Antibodies Used in Immunocytochemistry. Relates to Figure 4.

Marker	Catalog No.	Company	Dilution
p63α	4892S	Cell Signaling	1:100
K14	K14 Ab(Clone LL002)	NeoMarkers/Fisher Scientific	1:2
K12	Sc-25722	Santa Cruz Biotechnology	1:100

Transparent Methods

Based on the known small-molecule inhibitors that target the site 2 of Fzd8 CRD (Lee et al., 2015), the UNITY module in the Tripos software (Certara USA Inc, Princeton, NJ) was used to conduct an additional ligand-based screening against the ChemDiv (San Diego, CA) small-molecule library. A compound, ChemDiv compound 000A-099, which is 4-[2-[[9E]-2,7-dimethoxy-9H-fluoren-9-ylidene]hydrazin-1-yl]benzoic acid (termed as MFH), was identified as a potential Fzd binder. The compound was obtained from ChemDiv.

The consolidated compound, termed as MFH-ND, that links compound MFH to the ND peptide through a pentaethylene glycol ($(PEG)_5$) spacer was synthesized using standard solid phase Fmoc peptide chemistry; it was synthesized from the C-terminus to the N-terminus, starting from Fmoc-protected Lys attached to resin. Fmoc-protected amino acids and $(PEG)_5$ spacer were purchased from Anaspec (San Jose, CA, USA). MFH was added as the last segment and the synthesized compound cleaved from the resin with 90% trifluoroacetic acid (TFA, Sigma-Aldrich), 5% water, and 5% TIS for 2 h at room temperature.

Heteronuclear single quantum coherence spectroscopy nuclear magnetic resonance (HSQC NMR) experiments

The FZD8 CRD was subcloned and transformed into Rosetta2 (DE3) E. coli cells. The target protein, FZD8 CRD, was expressed by cells cultured in MOPS media supplemented with [^{15}N]ammonium chloride as the source of nitrogen. The protein was further purified by HPLC and maintained in 50 mM potassium phosphate at pH 6.5. Compound MFH was titrated into the solution of 50 µM FZD8 CRD for a final concentration of 276 µM. All spectra were recorded and analyzed as previously described (Lee et al., 2015) using ^{15}N-labeled protein on Bruker Avance

600 MHz NMR spectrometers equipped with ^{1}H/^{15}N detecting cryogenic inverse probes at 25°C. All spectra were processed using Topspin 3.0 NMR software (Bruker Biospin) and analyzed using the program CARA. To assign the backbone chemical shift of FZD8 CRD, 50 μM FZD8 CRD was prepared in 50 mM potassium phosphate, pH 6.5, and 10% D$_2$O (v/v). We performed two-dimensional ^{1}H-^{15}N HQSC (mix time = 120 ms) NMR experiments at 25°C. Chemical shift perturbation experiments were performed using ^{15}N-labeled FZD8 CRD. The two-dimensional ^{1}H-^{15}N HSQC spectra were recorded as a function of concentration of compound. The concentration of DMSO in the NMR titration experiment was below 3%. A control experiment was done by titrating 5% DMSO, which did not show any structural change in this condition.

Cell-based Wnt Luciferase Reporter Assay

Stably transfected HEK 293 (293STF) luciferase-based reporter cell line (ATCC, Manassas, VA), which expresses firefly luciferase under the control of TCF/LEF promoter, was used to examine the activation or inhibition effect of the small molecules (MFH-ND, MFH, and ND) on regulating the canonical Wnt signaling pathway. 293STF cells were cultured in 5% CO$_2$ at 37°C in Dulbecco's modified Eagle's medium supplemented with 4.5 g/L D-glucose and 2 mM glutamine (DMEM, Invitrogen, Carlsbad, CA) containing 10% fetal bovine serum (FBS, Invitrogen), 0.1 mM nonessential amino acids (Gibco), and 10 mM HEPES (Gibco). 293STF cells were seeded at 2x10^5 cells/well in a 96-well plate (Corning) and incubated overnight. NIH-3T3-J2 cells (from Howard Green, Harvard Medical School, Boston, MA, USA) were also transfected with the firefly luciferase under the control of the TCF/LEF promoter. NIH-3T3-J2 cells were cultured in 5% CO$_2$ at 37°C in DMEM supplemented with 10% bovine calf serum (BCS, HyClone) and 1% penicillin/streptomycin (Gibco). Cells were treated with vehicle (0.1% dimethyl sulfoxide

(DMSO); Sigma-Aldrich), 100-300ng/ml recombinant human Wnt3a protein (R&D), and Wnt3a with MFH-ND, MFH, or ND for 16 hours. Cell viability and firefly luciferase activity was measured using the ONE-Glo™ + Tox Luciferase Reporter and Cell Viability Assay kit (Promega, Madison, WI) following manufacturer's protocol. Microplate Reader, FilterMax F5 (Molecular Devices, Sunnyvale, California) was used to measure cell viability and firefly luciferase activity. The Wnt pathway activity was expressed as the ratio of fluorescence intensity to firefly luciferase. Experiments were performed in duplicate or triplicate.

Human corneoscleral tissue

Human corneoscleral tissue was from the Illinois Eye Bank (Watson Gailey, Bloomington, IL) and the Lions Eye Institute for Transplant and Research (Tampa, FL). Tissue donors were from 20 to 65 years old. No distinction was found based on the gender of the tissue donors. Experimentation on human tissue adhered to the tenets of the Declaration of Helsinki. The experimental protocol was evaluated and exempted by the University of California, Los Angeles Institutional Review Boards. The tissues were preserved in Optisol (Chiron Ophthalmics, Inc., Irvine, CA) at 4ºC, and the death-to-preservation time was less than 8 hours.

Isolation and culture of human LSCs

Human limbal epithelial cells (LECs), which contain LSCs, were isolated from corneoscleral rims following the previous protocol (Nakatsu et al., 2011). In brief, the trabecular meshwork, iris, endothelium, residual blood vessels, Tenon's capsules, and conjunctiva were mechanically removed. The corneoscleral rims were then digested by 2.4 U/ml Dispase II (Roche, Indianapolis, IN) in SHEM5 growth medium (DMEM/F12 medium) (Gibco) supplemented with N-2 (Gibco), 2 ng/ml epidermal growth factor (EGF; Gibco), 8.4 ng/ml cholera toxin (Sigma-Aldrich), 0.5

μg/ml hydrocortisone (Sigma-Aldrich), 0.5% dimethyl sulfoxide (DMSO; Sigma-Aldrich), 5% fetal bovine serum (FBS, Invitrogen), penicillin/streptomycin (Invitrogen) and gentamicin/amphotericin B (Invitrogen) for 2 hours at 37°C. Limbal epithelial cell sheets were mechanically scraped from the limbus and further digested with 0.25% trypsin and 1 mM EDTA (Gibco) for 10 min at 37°C to obtain a single-cell suspension. LECs were seeded at a density of 200 cells/cm^2 on growth arrested NIH-3T3-J2 cells (3 x 10^4 3T3 cells/cm^2, from Howard Green, Harvard Medical School, Boston, MA, USA) and cultured in SHEM5 growth medium for 11-13 days before harvesting. The growth medium was refreshed every 2-3 days. The LECs from the same donor were used for different culture conditions in each experiment to minimize donor variation.

Colony-forming efficiency (CFE)

At the end of culture, the cells in the 6-well plates were fixed with 4% paraformaldehyde (Thermo Fisher Scientific) and stained with 0.5% rhodamine B (Sigma-Aldrich) for 15 min at room temperature. The CFE was calculated as the number of colonies divided by the number of LECs seeded.

Immunocytochemistry and quantitative analysis

Cultured LSCs were harvested by incubating in 2.4 U/ml Dispase II (Roche) in SHEM5 growth medium for 2 hours at 37°C, followed by treatment with 0.25% trypsin and 1 mM EDTA (Gibco) for 7 min at 37°C. Harvested cells were counted with a hemocytometer (Fisher Scientific, Hampton, NH), placed onto slides using a cytospin cytocentrifuge (Cytofuge; Fisher Scientific), and stored at -80°C until use. The slides were then fixed with 4% paraformaldehyde at room temperature for 10 min, washed with phosphate-buffered saline (PBS) 3 times, blocked and

permeabilized with PBS containing 1% bovine serum albumin (BSA) and 0.5% Triton X-100 (Sigma-Aldrich) for 30 min at room temperature, and incubated with the primary antibody in PBS containing 1% BSA and 0.1% Triton X-100 overnight at 4ºC in a moist chamber. Cells were washed with PBS 3 times, incubated with the secondary antibody in PBS containing 1% BSA and 0.1% Triton X-100 at room temperature for 1 h, washed with PBS 3 times, labeled with the nuclear stain Hoechst 33342 (4 µg/ml; Invitrogen) at room temperature for 15 min, washed with PBS 5 times, and mounted in Fluoromount medium (Sigma). The primary antibodies and their dilution ratios are listed in Table S1.

Images were taken by an all-in-one fluorescence microscope (Keyence BZ-X710, Osaka, Japan). The nuclear intensity of p63α was analyzed by Keyence BZ-X analyzer (Osaka, Japan).

Statistical analysis

Student's *t*-test was performed to analyze the data. Error bars represent the standard error of the mean (SEM). P values ≤ 0.05 were considered statistically significant.

Supplemental References

Lee, H.J., Bao, J., Miller, A., Zhang, C., Wu, J., Baday, Y.C., Guibao, C., Li, L., Wu, D., and Zheng, J.J. (2015). Structure-based Discovery of Novel Small Molecule Wnt Signaling Inhibitors by Targeting the Cysteine-rich Domain of Frizzled. J Biol Chem *290*, 30596-30606.

Nakatsu, M.N., Ding, Z., Ng, M.Y., Truong, T.T., Yu, F., and Deng, S.X. (2011). Wnt/beta-catenin signaling regulates proliferation of human cornea epithelial stem/progenitor cells. Invest Ophthalmol Vis Sci *52*, 4734-4741.